Available online at www.sciencedirect.com
SCIENCE DIRECT
Journal of Molecular Catalysis A: Chemical 249 (2006) 13–22
JOURNAL OF MOLECULAR CATALYSIS A: CHEMICAL
www.elsevier.com/locate/molcata

Catalytic and mechanistic study of lean NO_2 reduction by isobutane and propane over HZSM-5

Dongmei Zhao [a,c,*], Hanna Härelind Ingelsten [a,b], Magnus Skoglundh [a,b], Anders Palmqvist [a,b,**]

[a] *Competence Centre for Catalysis, Chalmers University of Technology, SE-412 96 Göteborg, Sweden*
[b] *Applied Surface Chemistry, Chalmers University of Technology, SE-412 96 Göteborg, Sweden*
[c] *Department of Chemistry, Göteborg University, Kemivaegen 10, SE-412 96 Göteborg, Sweden*

Received 28 July 2005; received in revised form 21 December 2005; accepted 22 December 2005
Available online 3 February 2006

Abstract

In this study, the selective catalytic reduction (SCR) of NO_2 by two saturated hydrocarbons, propane and isobutane, has been investigated over acidic zeolite HZSM-5. The activity for NO_2 reduction and the selectivity for N_2 formation correlate well with the intracrystalline acidity (Brønsted acid sites) of the zeolite. Isobutane is a more efficient reducing agent than propane due to its tertiary hydrogen being more readily activated than the secondary hydrogen in propane. In situ DRIFT step–response experiments with NO_2 and isobutane show formation of surface bound NO^+, isocyanate, unsaturated hydrocarbons and amine species. The NO^+ species seems to play an important role in the reduction of NO_2 probably by reacting with alkenes formed from carbenium ion adsorbates. These species likely form isocyanates, amine species and finally nitrogen.

Keywords: HZSM-5; Lean NO_x reduction; Propane; Isobutane; FTIR

1. Introduction

Today diesel and lean burn gasoline engines are attractive alternatives to the conventional Otto engine due to lower fuel consumption and hence lower CO_2 emissions. However, an important disadvantage with these alternatives is that they operate at high air-to-fuel ratios that give oxygen excess in the exhaust gas, and thus make it difficult to reduce NO_x ($NO + NO_2$) formed during the combustion. This calls for efficient techniques for lean NO_x reduction.

Iwamoto et al. [1,2] and Held et al. [3] found early that Cu-ZSM-5 is an active catalyst for reduction of NO by hydrocarbons in oxygen excess. Furthermore, Iwamoto et al. showed the synergetic effect of oxygen for the selective catalytic reduction of nitrogen oxides by hydrocarbons (HC-SCR). Hamada et al. [4–6] observed that a redox system is not essential for this reaction, and that acidic zeolites, as well as alumina are active for lean NO_x reduction although at higher temperatures. However, in general the NO_x conversion is low for HC-SCR catalysts and the active temperature range is narrow. By identifying the key factors that control the HC-SCR process, both the conversion and active temperature interval for NO_x reduction could however be improved. The mechanistic proposal that HC-SCR over zeolite-based catalysts proceeds via intermediates containing carbon–nitrogen bonds is now widely accepted. This has been shown by different categories of experiments [7–17], among which N_2 formation has been demonstrated from compounds of the intermediate types envisaged, under HC-SCR reaction conditions. Such intermediate compounds can be nitrosoalkanes or nitrocompounds (nitroalkanes and nitroalkenes). Nitrosoalkanes can be converted to N_2 via oximes, nitriles and NH containing species, over transition metal exchanged zeolites [18–25], and acidic zeolites [20,23]. Nitroalkanes and nitroalkenes can be converted to isocyanate, which subsequently can be hydrolyzed to NH species and further to N_2. This has been reported over, e.g. Co-ZSM-5 [17,26], Cu-ZSM-5 [27] and H-ferrierite [10]; however, the details of the reaction still remain unclear. Formation of ammonia has been demonstrated for some systems, e.g. H-ferrierite [10], H-Cu-ZSM-5 [28], H-MOR [29,30] and Pd-H-MOR [31], in which the NH_3-SCR reaction is proposed to be

* Corresponding author. Tel.: +46 31 772 2886; fax: +46 31 772 2853.
** Corresponding author. Tel.: +46 31 772 2961; fax: +46 31 160 062.
E-mail addresses: dongmei@chem.gu.se (D. Zhao), adde@chem.chalmers.se (A. Palmqvist).

1381-1169/$ – see front matter © 2006 Elsevier B.V. All rights reserved.
doi:10.1016/j.molcata.2005.12.033

the final step in the reaction pathway. Furthermore, a reaction between gas phase NO_x and nitrogen containing deposits has been suggested [15,16]. A large number of experiments show C, N and O, or C and N containing intermediates in the gas phase during the SCR reaction. Formation of HCN and/or HNCO was observed during the HC-SCR reaction with C_2H_4 and C_3H_6 over Cu-ZSM-5 [32–35]. Cyanogens were observed over Cu-ZSM-5 during HC-SCR using isobutane as the reducing agent [28], and various nitriles were detected using C_3 and C_4 alkanes over Fe-ZSM-5 [25]. Furthermore, acrylonitrile was observed over Cu/H-ZSM-5 [23] using propane, and over H-MOR [30] using propene. Nitroethene has also been reported using ethene and NO_2 over H-ferrierite [11].

Already in an early stage of the research NO_2 was recognized to have an important role in the first step of HC-SCR reactions [5]. The HC-SCR activity of acidic zeolites has been found to increase when NO_2 is used as NO_x source instead of NO [17]. This characteristic has been used to improve the SCR performance by combining two functionally different catalysts, the first being an NO oxidation catalyst and the second an active catalyst for the SCR of NO_2 [36,37]. The dual pore system catalyst concept is also based on this strategy, but with two different types of zeolites mixed in one catalyst [38,39].

A possible reaction pathway for lean NO_2 reduction by propane over HZSM-5 has been presented previously [40]. The key initiating steps are likely the formation of NO^+ species on the catalyst surface and the activation of the hydrocarbon over Brønsted acid sites, forming carbenium ion adsorbates and subsequently alkenes. A reaction between the alkenes and the NO^+ species may form oximes (R-CNO), which can easily be rearranged to isocyanate species (R-NCO) [41]. Hydrolysis of the isocyanate species with water can thus form amine species, which may in turn react with the NO^+ species, or with NO_2 in the gas phase, forming N_2. In the present study we focus on the selective catalytic reduction of NO_2 by propane and isobutane over a series of HZSM-5 samples with varying SiO_2/Al_2O_3 ratio. The objective is to study the activity and reaction mechanism for lean reduction of NO_2 correlated with the type of hydrocarbon and the surface acidity.

2. Experimental

2.1. Catalyst preparation

The catalysts used in this study were HZSM-5 zeolites, received from Albemarle Catalysts BV, with different SiO_2/Al_2O_3 molar ratios (40, 234 and 569), denoted HZSM-5(40), HZSM-5(234) and HZSM-5(569), respectively. The textural properties of the samples are shown in Table 1. The samples were pressed into discs, and then ground and sieved to obtain a size fraction between 300 and 500 μm.

2.2. Activity studies

The catalytic activity for NO_x reduction and the selectivity for N_2 formation were investigated in a vertical flow reactor (21 mm i.d., 58 cm long quartz tube with a thin sintered quartz filter disc fused into the tube 28 cm from the upper end). The reactor was heated by a tubular furnace (controlled by Eurotherm 818S) and the temperature was measured using a thermocouple (K-type) located inside the reactor, 2 mm above the catalyst bed. This reactor system is also described in detail previously [40]. The catalytic samples were pre-conditioned for 30 min at 500 °C in a gas composed of 10% O_2 (99.9996%) in helium (99.9996%) before exposure to the reactants. The gas flow was controlled by separate mass flow controllers, and the total flow rate was maintained constant at 1500 ml (NTP)/min corresponding to a space velocity of about 50,000 h^{-1}. The inlet feed composition was 10% O_2 (99.9996%), 1040 ppm NO_2 (0.983% in He) and 300 ppm propane (2% in He) or 200 ppm isobutane (2% in He), balanced with helium. The reaction temperature was decreased step-wise (100 °C/step) from 650 to 350 °C for C_3H_8 and from 450 to 250 °C for *i*-C_4H_{10}. The products were monitored on-line, and NO_x (i.e. the sum of NO and NO_2) and NO were determined by an Eco Physics, CLD 700 EL ht chemiluminescence analyzer. Nitrogen dioxide was calculated from the measured NO_x and NO concentrations. An Agilent 6850 gas chromatograph fitted with a HP-PLOT Molesieve column and a thermal conductivity detector was used to quantify N_2. Water, CO_2, NO_x and unreacted hydrocarbons were removed by a liquid nitrogen cooled cold trap, located upstream of the gas chromatograph. Carbon monoxide, CO_2 and N_2O were measured by photo acoustic FTIR spectroscopy, employing a Bruel & Kjaer, Type 1301 analyzer. Other possible nitrogen containing reaction products, if present, could be detected by the same technique.

The catalyst performance was studied under steady state conditions at each temperature, which was achieved within around 10 min after changing conditions. At each steady state condition, the catalysts were exposed to the reactants for about 1 h to complete the measurement for all the components. The catalysts were stable during the entire experiment.

Table 1
Textural properties of the HZSM-5 zeolites used in the experiments

	HZSM-5(40)	HZSM-5(234)	HZSM-5(569)
Crystallinity (%)	95	98	100
SiO_2/Al_2O_3	39.7	234	569
Na_2O (wt%)	<0.05	0.01	0.03
MiPV[a] (ml/g)	0.177	0.183	0.183
SA[b] (m^2/g)	405	407	377

[a] Micropore volume.
[b] BET surface area.

2.3. In situ DRIFT studies

The in situ Fourier Transform Infrared (FTIR) spectroscopy measurements were carried out using a BioRad FTS 6000 spectrometer in diffuse reflection (DRIFT) mode, equipped with a continuous flow reactor chamber with KBr windows (Harrick Scientific Praying Mantis DRIFT cell). The set-up is described in detail elsewhere [42,43]. About 30 mg of the calcined zeolite sample was placed on a tungsten grid (6.2 mm × 3.2 mm), which is situated over the outlet of the reaction chamber. The temperature was measured with a K-type thermocouple. The

gases, Ar (99.995%), O_2 (99.95%), NO_2 (5000 ppm in Ar), C_3H_8 (1% in Ar) and isobutane (2% in Ar), were introduced via mass flow controllers (Bronkhorst Hi-Tech) to the DRIFT cell. The samples were initially pre-treated in nitrogen dioxide and oxygen (1000 ppm NO_2 and 10% O_2, balanced with Ar, 500 °C, 40 min) followed by oxygen (10% O_2 in Ar, 500 °C, 1 h) and then flushed in pure Ar (500 °C, 15 min) at a total flow rate of 300 ml (NTP)/min (the flow rate was kept constant throughout the experiments). Background spectra (40 scans at a resolution of 1 cm^{-1}) were collected for each temperature, under Ar exposure. Fresh samples were used for all experiments.

In situ reaction experiments were performed for the samples HZSM-5(40) and HZSM-5(234) with isobutane as reducing agent. The samples were pre-treated and the background spectra were recorded as mentioned before. The reaction experiments were performed in three sequences. Sequence 1, feeding 1000 ppm NO_2 and 10% O_2 in Ar to the DRIFT cell, the co-adsorption of O_2 and NO_2 on the catalyst surface was recorded in the spectra as a function of time (typically 0, 20 s, 1, 2, 3, 5, 7, 10, 15 and 20 min or until saturation). Sequence 2, the reducing agent, isobutane, was added to the feed; thus, the reaction $NO_2 + O_2$ + isobutane started over the catalyst and IR spectra were recorded as a function of time. Sequence 3, when the reaction in sequence 2 reached steady state, the supply of reducing agent was switched off, leaving the sample only exposed to NO_2 and O_2, and new spectra were recorded as a function of time.

3. Results

3.1. Evaluation of the catalytic activity

3.1.1. Characterization of surface acidity

The surface acidity was investigated using DRIFT spectroscopy under Ar exposure (Fig. 1). The absorption peaks at 3737 and 3600 cm^{-1} are assigned to O–H stretching vibrations originating from silanol groups (Si–OH) and Si(OH)Al bridging hydroxyl groups, respectively [23,44–50]. The results clearly demonstrate the difference in acidity between the different samples. The sample with higher alumina content, HZSM-5(40), contains significant amounts of Brønsted acid sites, whereas the other two samples, HZSM-5(234) and HZSM-5(569), contain considerably less or negligible amounts of these sites. Detailed results from ammonia adsorption experiments, over these samples, have been reported in a previous paper [40].

3.1.2. Influence of surface acidity on the NO_x conversion

Figs. 2a and 3a show the NO_x conversion over the catalysts, HZSM-5(40), HZSM-5(234) and HZSM-5(569), for SCR of NO_2 with isobutane and propane, respectively, as a function of temperature, allowing about 10 min to reach steady state at each temperature.

For isobutane (Fig. 2a), the highest activity for NO_x reduction is obtained with the HZSM-5(40) sample at 350 °C, followed, in decreasing order of activity, by HZSM-5(234) and HZSM-5(569). When using propane as the reducing agent, the same order of activity is observed for the maximum NO_x conversion (Fig. 2b) at 450 °C for the three samples. These results indicate that the Brønsted acidic sites most likely are the active sites for this reaction and that the HC-SCR activity is related to the amount of acidic sites. This is in accordance with previous reports both on non-zeolite catalysts [6,43,51] and acidic zeolites [4,5,40]. Moreover, as shown in Figs. 2a and 3a, the maximum conversion of NO_x is observed over the HZSM-5(40) sample, both for isobutane and propane, however, at different temperatures, 350 °C for isobutane and 450 °C for propane. Furthermore, isobutane exhibits higher maximum NO_x conversion (54%) than propane (39%).

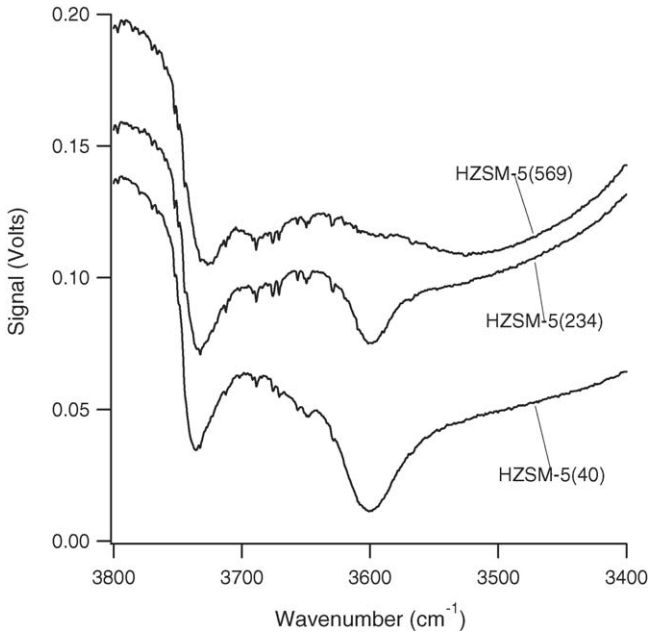

Fig. 1. FTIR spectra of the three different HZSM-5 samples collected at steady state during Ar flow at 350 °C. The measured signals of the baselines are off-set by −0.04, −0.01 and 0.03 V, respectively, for clarity.

When relating the conversion of NO_x over the three samples with their aluminum content, which may be assumed to correspond to the number of Brønsted acid sites, it seems that the activity per site is somewhat higher for the samples with the higher SAR, indicating higher turn-over frequencies over these samples. This is possibly related to differences in the strength of the acid sites between the samples. However, the purpose of the sample comparison was to find the sample giving the highest conversion of NO_x and for this reason it appears that the total acidity is of greater importance making the HZSM-5(40) sample the one showing highest overall conversion.

3.1.3. Dependence of product selectivity on the type of hydrocarbon

Since the HZSM-5(40) sample gave the highest NO_x conversion among the catalysts studied, the following studies were focused on this catalyst. Figs. 2b and 3b show the conversion of NO_2 and hydrocarbon (isobutane or propane), and the selectivity for N_2 and NO formation as a function of temperature.

The NO_2 conversion in percent is defined as:

$$C_{NO_2\,conv.} = \frac{100 \times n_{NO_2\,conv.}}{n_{NO_2\,add.}}$$

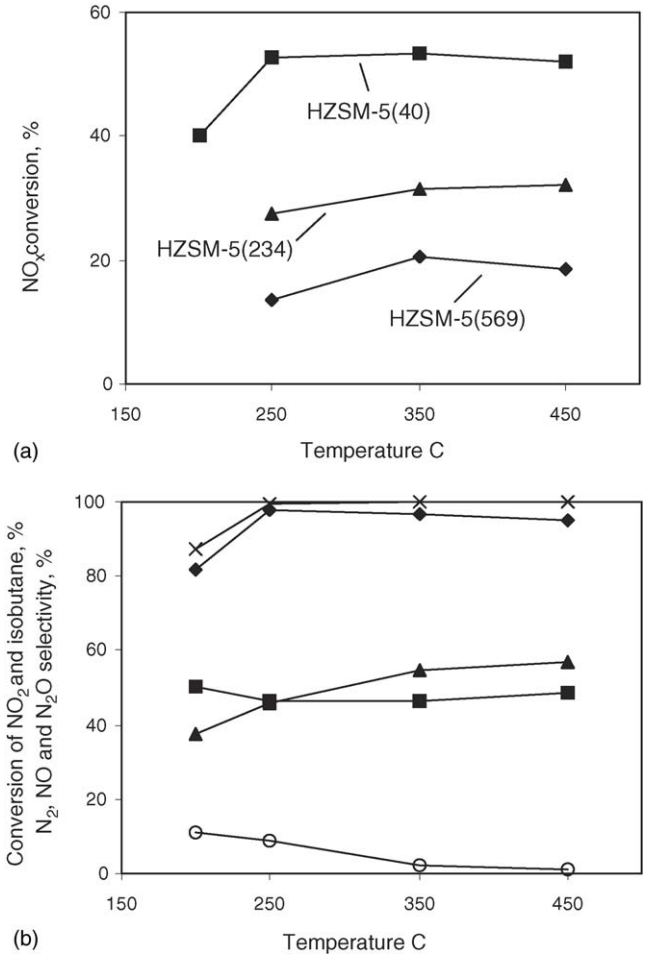

Fig. 2. (a) Temperature dependence of the NO_x conversion in the SCR of NO_2 with isobutane over a series of acidic HZSM-5 samples. HZSM-5(40) (squares), HZSM-5(234) (triangles) and HZSM-5(569) (diamonds). (b) Temperature dependence of the conversion of NO_2 (diamonds) and isobutane (crosses), and the selectivity of N_2 (triangles), NO (squares) and N_2O (circles), in the SCR reaction of NO_2 with isobutane over the HZSM-5(40) sample. Gas composition: 200 ppm isobutane, 1040 ppm NO_2, 10% O_2 in He, total flow 1500 ml (NTP)/min.

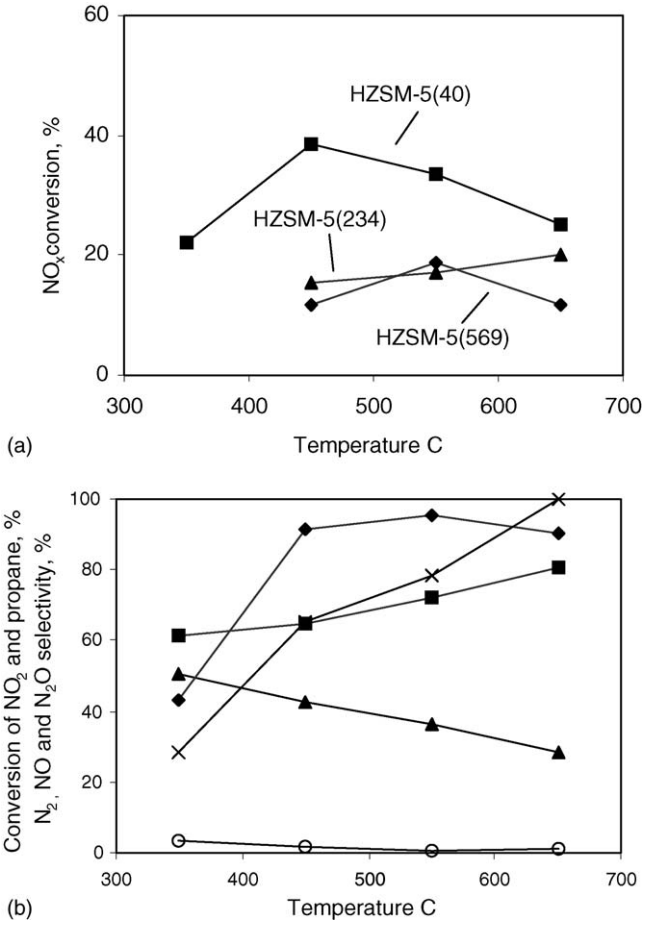

Fig. 3. (a) Temperature dependence of the NO_x conversion in the SCR of NO_2 with propane over a series of acidic HZSM-5 samples. HZSM-5(40) (squares), HZSM-5(234) (triangles) and HZSM-5(569) (diamonds). (b) Temperature dependence of the conversion of NO_2 (diamonds) and propane (crosses), and the selectivity of N_2 (triangles), NO (squares) and N_2O (circles), in the SCR reaction of NO_2 with propane over the HZSM-5(40) sample. Gas composition: 300 ppm propane, 1040 ppm NO_2, 10% O_2 in He, total flow 1500 ml (NTP)/min.

where $n_{NO_2\,conv.}$ is the number of NO_2 molecules converted and $n_{NO_2\,add.}$ is the number of NO_2 molecules added.

The hydrocarbon conversion in percent is defined as:

$$C_{HC\,conv.} = \frac{100 \times n_{HC\,conv.}}{n_{HC\,add.}}$$

where $n_{HC\,conv.}$ is the number of hydrocarbon molecules converted and $n_{HC\,add.}$ is the number of hydrocarbon molecules added.

The N_2, NO and N_2O selectivity in percent is defined as:

$$S = \frac{100 \times n_{form.} \times n}{n_{NO_2\,conv.}},$$

where $n_{form.}$ is the number of N_2, NO or N_2O molecules formed, n the number of nitrogen atoms in the molecule and $n_{NO_2\,conv.}$ is the number of NO_2 molecules converted.

As shown in Figs. 2b and 3b, the conversion of NO_2 reached about 95% or higher with isobutane and 90% or higher with propane as the reductant, however in different temperature regions (250–450 °C for isobutane and 450–650 °C for propane). The selectivity to N_2 increased slightly (from 46 to 57%) in the active temperature range for i-C_4H_{10}, while the corresponding value for propane decreased (from 51 to 29%) with increasing temperature. The selectivity to NO was approximately constant (increased from 47 to 48%) for isobutane and increased (from 61 to 81%) for propane in their respective active temperature range. The change in NO selectivity corresponds well with the change in selectivity to N_2. This indicates that the main N containing products in the reaction are NO and N_2. Some N_2O formation was also observed during the reaction, but the concentration was low or negligible (below 20 ppm) at temperatures of 350 °C and above, whereas at 200 and 250 °C somewhat higher N_2O concentrations were obtained in the isobutane case. The conversion of hydrocarbons appeared to be different for isobutane and propane. Isobutane was converted to almost 100% within its active temperature range (250–450 °C), while the conversion of propane was only 62% at 450 °C, which subsequently increased to 100% when the temperature reached 650 °C. The conversion

of i-C_4H_{10}, which correlates with the corresponding slightly decreased NO_x conversion for i-C_4H_{10} (Fig. 2a) over the same temperature range, indicates that the reaction mainly occurs between NO_x and i-C_4H_{10}. This is verified by the selective formation of N_2, which increased in the same active temperature range. However, within the active temperature range for propane, the NO_x reduction over the HZSM-5(40) sample actually decreased; hence, the higher conversion of propane at higher temperatures was most likely caused by reaction with oxygen. This correlates well with the N_2 formation, which decreased in the corresponding temperature range. From this it follows that isobutane is effectively activated at lower temperatures (250 °C) compared to propane and that the reaction with NO_2 is favored rather than the oxidation with oxygen. This results in a wider active temperature window (250–450 °C) in NO_x reduction for isobutane compared to propane for which high activity for NO_x reduction appeared only around 450 °C.

3.1.4. Reaction products and possible reaction intermediates

There are several reports in the literature, where C, N and O containing species have been observed as by-products in the gas phase (such as HCN, HNCO, NH_3, etc.) during the SCR reaction. The gas phase FTIR spectra recorded in this study during the activity experiments over the HZSM-5(40) sample are shown in Fig. 4, at 250, 350 and 450 °C. Even though the exact structures of some of the molecules involved in these spectra are uncertain, the characteristic absorption peaks of different functional groups can be recognized. The peaks at 1630 and 1595 cm^{-1} typically originate from asymmetric stretching of the NO_2 group and the peaks at 2915 and 2885 cm^{-1}, from the C–H stretching of isobutane. The main products CO_2 (peaks at 2355 and 2360 cm^{-1}) and NO (peaks at 1890 and 1830 cm^{-1}) are observed at all temperatures investigated. The two doublets at 2100 and 2165 cm^{-1} and at 2200 and 2210 cm^{-1} are typically CO and N_2O absorption peaks [52]. The intensity of the CO peaks is stronger when the temperature is higher, indicating more CO formation at higher temperatures (Fig. 4). Meanwhile, the N_2O formation is higher at low temperatures and negligible at higher temperatures. Furthermore, peaks in the N–H stretching region, 3200–3400 cm^{-1}, which are more pronounced at 350 °C, may indicate formation of organic amine species. The peak at 3180 cm^{-1}, which likely originates from the alkene C–H stretching, indicates formation of alkenes. Species like HCN, HNCO and/or NH_3 were not observed during these experiments.

The corresponding gas phase FTIR spectra for the HZSM-5(234) sample are shown in Fig. 5, at 250, 350 and 450 °C. The NO_2, CO_2 and NO are observed by the presence of their characteristic peaks, as described previously for the HZSM-5(40) sample. The peaks for CO and N_2O change in a similar way as observed for the HZSM-5(40) sample, i.e. at lower temperature the N_2O formation is higher. The intensity of the N–H stretching peaks (3200–3400 cm^{-1}) is similar to that observed for the HZSM-5(40) sample (gas phase). Formation of HCN and NH_3 could not be observed. However, there is a shoulder at 2280 cm^{-1} (Fig. 5) appearing at 250 °C in the spectrum, typical for the –NCO group in gas phase, which may indicate the presence of HNCO or –NCO species.

3.2. In situ DRIFT studies; formation of surface bound species

The mechanism of lean NO_2 reduction with isobutane was studied by in situ DRIFT step–response experiments. Below 2000 cm^{-1} the background noise level is high, which makes identification of the peaks difficult. This noise is probably related to perturbed vibration frequencies of the zeolite framework [49,50,53].

3.2.1. Co-adsorption of NO_2 and O_2

Fig. 6a shows the DRIFT spectrum of reaction sequence 1, after introduction of 1000 ppm NO_2 and 10% O_2 over the

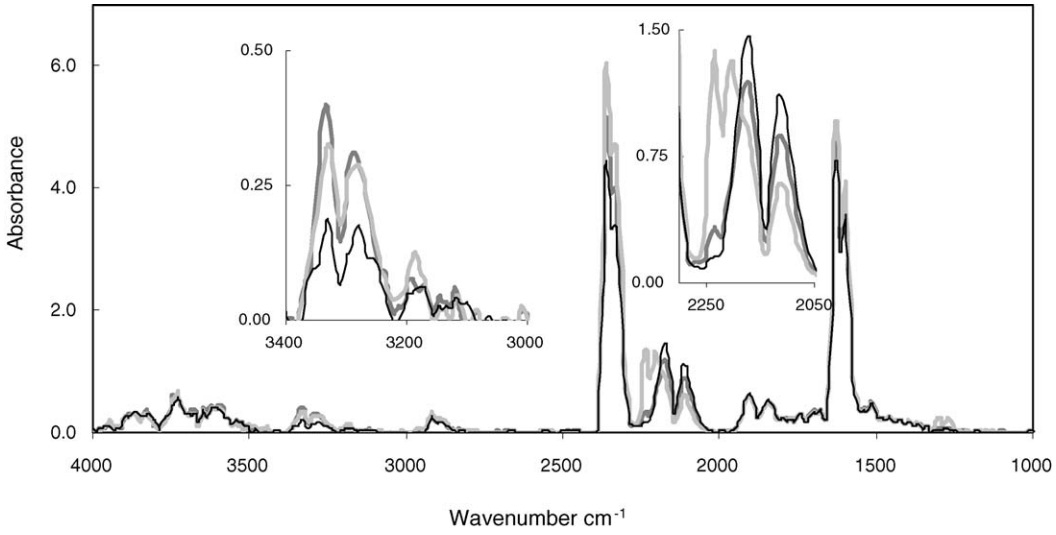

Fig. 4. Gas phase IR spectra recorded at 250 °C (light grey), 350 °C (grey) and 450 °C (black) during activity experiments over the HZSM-5(40) sample. Gas composition: 1040 ppm NO_2, 200 ppm isobutane and 10% O_2 in He. The insets represent enlargement of the 3400–3000 and 2250–2050 cm^{-1} regions, characteristic for N–H and unsaturated C–H stretching vibrations, and for isocyanates, N_2O and CO, respectively.

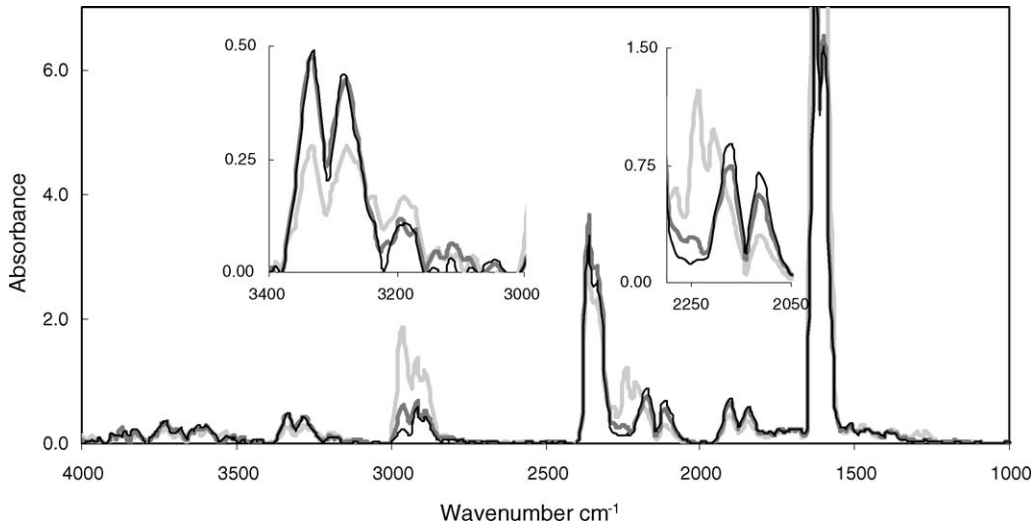

Fig. 5. The gas phase IR spectra recorded at 250 °C (light grey), 350 °C (grey) and 450 °C (black) during the activity experiments over the HZSM-5(234) sample. Gas composition: 1040 ppm NO_2, 200 ppm isobutane and 10% O_2 in He. The insets represent enlargement of the 3400–3000 and 2250–2050 cm^{-1} regions, characteristic for N–H and unsaturated C–H stretching vibrations, and for isocyanates, N_2O and CO, respectively.

HZSM-5(40) sample at 250 °C. A positive peak at 2140 cm^{-1} appears and its intensity grows with time. This peak has been assigned, by Hadjiivanov et al. [44], to adsorbed NO^+ species. Negative peaks at 3610 and 3745 cm^{-1} are also observed, which are assigned to O–H stretching vibrations originating from Brønsted acid sites and silanol groups, respectively [44–50]. The negative peak at 3610 cm^{-1} reflects the NO^+ groups, which are mainly adsorbed on Brønsted acid sites. Two broad peaks, centred around 2880 and 2490 cm^{-1}, appear which probably originate from the perturbed O–H stretching vibrations caused by hydrogen bonds with H in the OH group [49]. The NO_2/O_2 experiment was repeated at 350 °C, and the same peaks at 2140, 3610 and 3745 cm^{-1} are observed in the spectrum (Fig. 6b), though with lower intensity, except for the two broad water peaks, which almost disappeared due to higher temperature.

The corresponding spectra (Fig. 6c) for the HZSM-5(234) sample showed the same positive NO^+ peak at 2140 cm^{-1}; however, its steady state intensity was much lower compared to the HZSM-5(40) sample at 350 °C. The weaker intensity is likely due to the lower number of Brønsted acid sites present in this sample. No broad zeolite hydroxyl peaks are observed at this temperature.

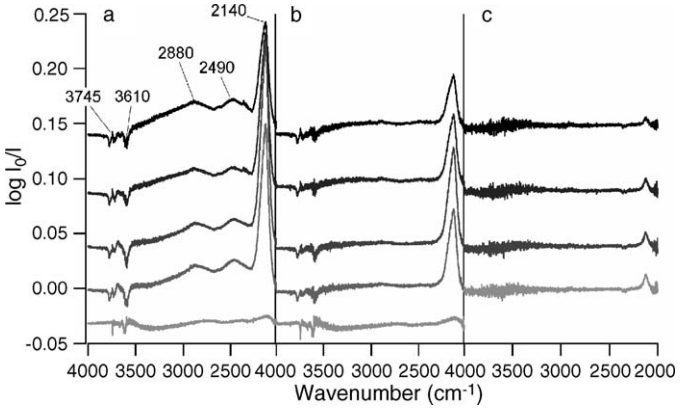

Fig. 6. DRIFT experiments with 1000 ppm NO_2 and 10% O_2 in Ar (sequence 1). Light grey corresponds to time direct after the gas switch and time is then increased until steady state is reached, which is illustrated with black. (a) HZSM-5(40) at 250 °C, (b) HZSM-5(40) at 350 °C and (c) HZSM-5(234) at 350 °C. For clearance the log I_o/I values have been off-set.

3.2.2. *Reduction of NO_2 by isobutane*

Fig. 7a shows the step–response DRIFT experiments when 200 ppm isobutane is introduced to the mixture of 1000 ppm NO_2 and 10% O_2 over the HZSM-5(40) sample at 250 °C (sequence 2). A broad feature evolves in the 3500–2000 cm^{-1} region in which also more narrow peaks develop. The growth of the two broad peaks, centred around 2880 and 2490 cm^{-1}, indicates the formation of water from the reaction. The presence of the peaks in the range 2000–2300 cm^{-1} suggests formation of new species containing double bonds (e.g. –N=C=O) or triple-

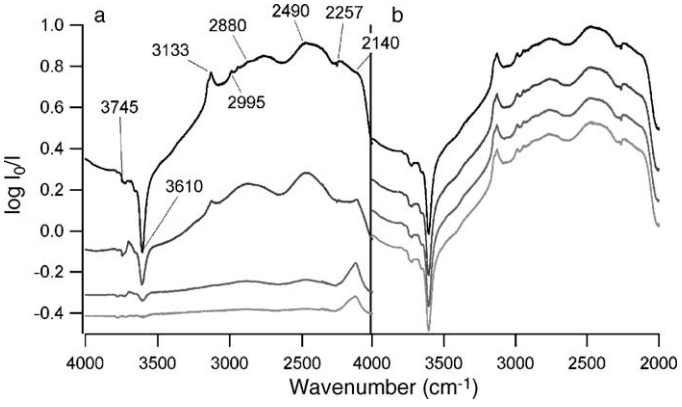

Fig. 7. Step–response DRIFT experiments over the HZSM-5(40) sample at 250 °C, using isobutane as the reducing agent. Light grey corresponds to time direct after the gas switch and time is then increased until steady state is reached, which is illustrated with black. (a) Isobutane is turned on; 1000 ppm NO_2, 200 ppm C_4H_{10}, 10% O_2 in Ar (sequence 2). (b) Isobutane is turned off; 1000 ppm NO_2, 10% O_2 in Ar (sequence 3). For clearance the log I_o/I values have been off-set.

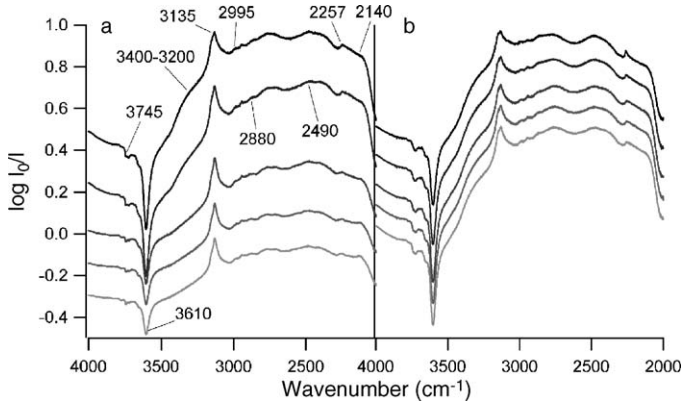

Fig. 8. Step–response DRIFT experiments over the HZSM-5(40) sample at 350 °C, using isobutane as the reducing agent. Light grey corresponds to time direct after the gas switch and time is then increased until steady state is reached, which is illustrated with black. (a) Isobutane is turned on; 1000 ppm NO_2, 200 ppm C_4H_{10}, 10% O_2 in Ar (sequence 2). (b) Isobutane is turned off; 1000 ppm NO_2, 10% O_2 in Ar (sequence 3). For clearance the log I_o/I values have been off-set.

bonds (e.g. –C≡N and –C≡C) [46]. Peaks at 2257 cm^{-1} are often assigned to isocyanate (–N=C=O) and/or nitrile (–C≡N) species [16,23,50,54–56]. The assignment of peaks in this region to adsorbed species with well defined structure is difficult because cyanides, isocyanides, cyanates, isocyanates and carbonyl all exhibit strong IR peaks between 2300 and 2000 cm^{-1} [56]. The 2140 cm^{-1} (NO^+) peak is observed as a shoulder growing on the large feature. There are indications of peaks growing in the 2500–2400 cm^{-1} region, which may be due to *t*-butylnitrile N-oxide [41], but could also be assigned to bidentate nitrate [23]. In the region 3000–2800 cm^{-1}, C–H stretching vibrations occur [16,23,57]. In particular, a peak at 2950 cm^{-1} can probably be attributed to isobutane [24] (in gas phase or loosely bound to the surface), and a peak at 2995 cm^{-1} can be due to presence of *t*-butyl groups [58]. A clear peak appears and develops with time at 3133 cm^{-1}, which can be assigned to C–H stretching vibrations of unsaturated hydrocarbons [16,24] and/or N–H stretching vibrations of amine species or ammonia [24,59,60]. There are also indications of a shoulder in the region 3400–3200 cm^{-1}, which probably originates from N–H stretching vibrations [16,23,24,28,61]. Moreover, the concomitant increase in intensity of the negative peaks at 3745 and 3610 cm^{-1} implies adsorbates on the Brønsted OH groups, likely isobutane. The experiment was repeated over the same catalyst at 350 °C and the results are shown in Fig. 8a. In the large feature region, 3500–2000 cm^{-1}, the two broad zeolite hydroxyl peaks appear more flat than at 250 °C indicating less adsorption of water at this temperature. All the other peaks described for 250 °C were observed also at 350 °C. The shoulder that appears in the NH stretching region (3400–3200 cm^{-1}) is much more pronounced at 350 °C than at 250 °C, indicating that more –NH surface species are formed at this temperature. At both temperatures the isocyanate species (2257 cm^{-1}) and the unsaturated hydrocarbons and/or amine species (3135 cm^{-1}) increase immediately after isobutane has been introduced. At the same time the Brønsted acid sites are blocked, likely by these species (Fig. 9).

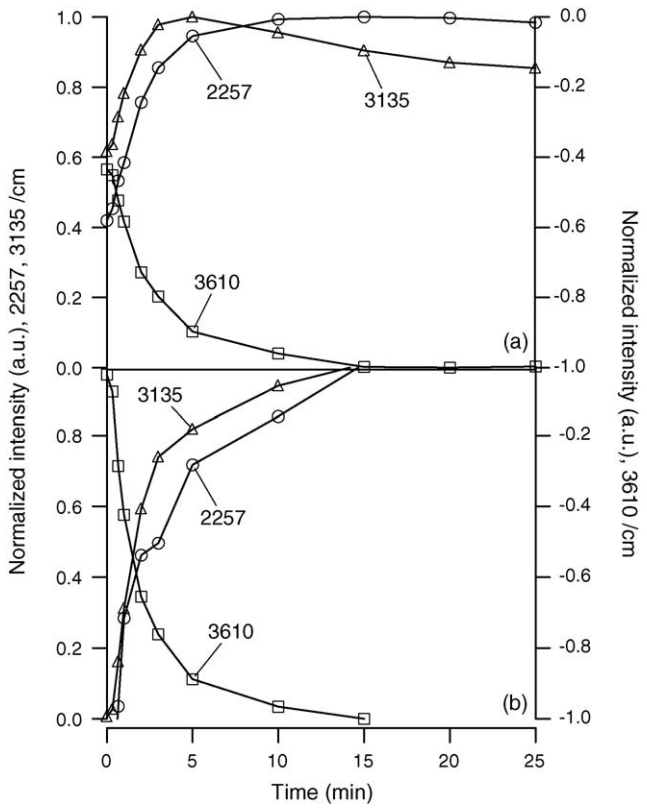

Fig. 9. Intensity variation with time for isocyanate species (2257 cm^{-1}), amine species and/or unsaturated hydrocarbons (3135 cm^{-1}) and Brønsted acid sites (3610 cm^{-1}), when 200 ppm isobutane is added to the reaction gas mixture (1000 ppm NO_2 and 10% O_2) at: (a) 350 °C and (b) 250 °C. The values are normalized between 0 and 1, and between −1 and 0, respectively.

At 350 °C the 3135 cm^{-1} peak reaches a maximum where after it decreases. This is possibly related to the water formation in the reaction. Isocyanate species are proposed to hydrolyze with water forming amine species; however, the water is likely consumed initially and the formation may not be sufficient for a total hydrolysis of isocyanate species.

In Fig. 10 the results from the NO_2 reduction with isobutane over the HZSM-5(234) sample at 350 °C are shown. The results are similar to the results for the HZSM-5(40) sample with the –NCO and/or –CN (peak at 2257 cm^{-1}) species growing, and the Brønsted acid sites (peaks at 3610 cm^{-1}) becoming increasingly affected with time. However, there is a large difference in the intensities of the peaks, which are much weaker for the HZSM-5(234) sample compared to the HZSM-5(40) sample, as a result of less adsorbed species on the catalyst surface.

3.2.3. Reactivity of the adsorbed complexes formed during NO_2 reduction

The chemical stability of the adsorbed reaction complexes over HZSM-5(40) towards NO_2 has been investigated (sequence 3). When the NO_2 reduction has reached steady state in sequence 2, the supply of isobutane was turned off, still allowing $NO_2 + O_2$ through the sample (sequence 3). This sequence was performed both at 250 and 350 °C, and the results are shown in Figs. 7b and 8b, respectively. The light grey line represents the

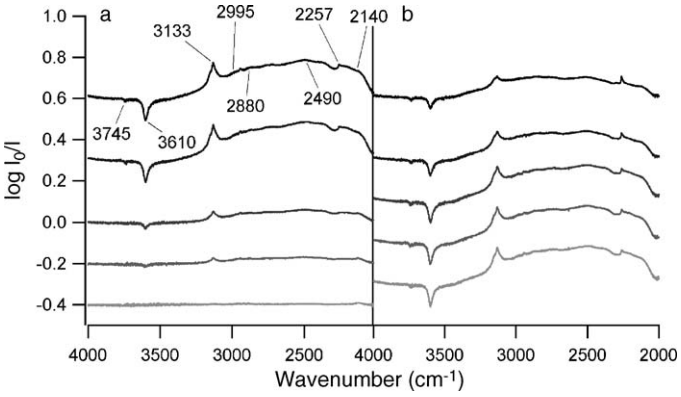

Fig. 10. Step–response DRIFT experiments over the HZSM-5(234) sample at 350 °C, using isobutane as the reducing agent. Light grey corresponds to time direct after the gas switch and time is then increased until steady state is reached, which is illustrated with black. (a) Isobutane is turned on; 1000 ppm NO_2, 200 ppm C_4H_{10}, 10% O_2 in Ar (sequence 2). (b) Isobutane is turned off; 1000 ppm NO_2, 10% O_2 in Ar (sequence 3). For clearance the $\log I_0/I$ values have been off-set.

reaction at steady state (sequence 2), which is the starting point of the exposure to $NO_2 + O_2$, and the black line represents the end of the exposure, at which no more change can be observed in the spectra. As can clearly be seen, the reaction complex formed at 250 °C is chemically very stable towards gas phase NO_2, since no changes are observed in the DRIFT spectra (Fig. 7b) after 5 min exposure to NO_2 in 10% O_2. However, at 350 °C, as shown in Fig. 8b, some peaks decrease in intensity. The two broad hydroxyl peaks centred at 2490 and 2880 cm^{-1} decrease to a certain extent and the isocyanate (–NCO) and/or nitrile (–CN) peak at 2257 cm^{-1}, and the NO^+ peak at 2140 cm^{-1} decrease correspondingly. This may indicate that the adsorbed isocyanate and/or nitrile species on the surface are hydrolyzed with trace amounts of adsorbed water (formed on the surface during the reaction) and the hydrolysis products likely react with NO^+ species [25], leading to a decrease in the NO^+ peaks. When the adsorbed water is mostly consumed, the hydrolysis reaction ceases and no more decrease in intensity can be observed. The remaining peaks likely originate from hydrocarbons or derivatives of hydrocarbons hydrogen-bonded to the zeolite hydroxyl groups. The peak at 3135 cm^{-1}, originating from C–H stretching vibrations of unsaturated hydrocarbons, only slightly decreases in intensity, and the negative peak at 3610 cm^{-1} was also slightly decreased in intensity implying a slight recovery of Brønsted acid sites.

The corresponding results obtained for the HZSM-5(234) sample at 350 °C are shown in Fig. 10b. The light grey line represents the start of the exposure to $NO_2 + O_2$ (in Ar) and the black line represents the end of the exposure, at which no more changes are observed in the spectra. The changes are more pronounced for this sample compared to HZSM-5(40). The intensity of the two broad bands (centred around 2490 and 2880 cm^{-1}), the nitrile and/or isocyanate species (peak at 2257 cm^{-1}) and NO^+ species (2140 cm^{-1}) decreases with time. The decrease may be caused by the hydrolysis of –CN/–CNO species with trace amounts of adsorbed water, and the reaction of hydrolysis products with NO^+ species. Even though less amounts of complexes are adsorbed on the catalyst surface, the complexes seem to be more reactive than over the HZSM-5(40) sample. This is indicated by less blockage of hydrocarbons over this sample and further supported by the =C–H peaks at 3133 cm^{-1}, which decrease with time upon exposure to $NO_2 + O_2$. The negative peak at 3610 cm^{-1}, originating from the Brønsted acid sites, decreased considerably more compared to the change over the HZSM-5(40) sample, indicating a higher recovery of active Brønsted acid sites.

4. Discussion

In a previous study, we investigated the reaction mechanism for NO_2 reduction by propane, as an example for saturated hydrocarbons, over acidic HZSM-5 zeolites [40]. The present study focuses on the differences in NO_2 SCR activity between two saturated hydrocarbons: propane and isobutane and on the reaction mechanism for NO_2 SCR with isobutane.

The HZSM-5(40) sample shows the highest NO_x conversion and the highest N_2 formation for all temperatures studied and for both reducing agents (isobutane and propane) due to its higher content of Brønsted acid sites. Moreover, the present study shows that the NO_2 reduction in O_2 excess is dependent on the type of hydrocarbon used. Over the most active HZSM-5(40) sample, isobutane was effectively activated at 250 °C, and the effectiveness, by which isobutane reduces NO_x, was sustained over a wider temperature range compared to propane.

The influence of mass transfer limitations on the reduction of NO_x is considered by estimating the Weiszs-modulus [62], in accordance with calculations presented previously [40], and the results are shown in Table 2. This estimation compares the reaction rate and the diffusion rate of the reactants at the active surface. When the reaction rate is high, the reaction can essentially take place in the first small part of the catalyst bed, and hence there may be transport limitations in this part of the catalyst bed. In most cases of the present study, the catalytic reaction

Table 2
The values used for estimation of the Weiszs-modulus at 450 °C for propane and at 350 °C for isobutane

	Propane		Isobutane	
	r_{obs} (mol/(s kg_{cat}))	Φ	r_{obs} (mol/(s kg_{cat}))	Φ
HZSM-5(40)				
$NO_{2\,cat.part.}$	4.0E−04	0.43	5.75E−04	0.53
$NO_{2\,zeolite.part.}$	6.1E−04	0.52	8.84E−04	0.65
$HC_{cat.part.}$	2.1E−04	0.77	2.07E−04	0.99
$HC_{zeolite.part.}$	3.2E−04	0.95	3.18E−04	1.22
HZSM-5(234)				
$NO_{2\,cat.part.}$	1.7E−04	0.18	3.39E−04	0.31
$NO_{2\,zeolite.part.}$	2.6E−04	0.23	5.21E−04	0.38
$HC_{cat.part.}$	1.2E−04	0.44	1.67E−04	0.80
$HC_{zeolite.part.}$	1.8E−04	0.54	2.57E−04	0.99
HZSM-5(569)				
$NO_{2\,cat.part.}$	1.4E−04	0.15	2.20E−04	0.20
$NO_{2\,zeolite.part.}$	2.1E−04	0.18	3.38E−04	0.25
$HC_{cat.part.}$	3.5E−05	0.13	8.47E−05	0.41
$HC_{zeolite.part.}$	5.4E−05	0.16	1.30E−04	0.50

is likely not influenced by mass transfer limitations. This means that the diffusion of the reactants, i.e. NO_2 and propane or isobutane, to the active sites within the zeolite channels [63] does not limit the SCR reaction. However, in four cases the values of the Weiszs-modulus are close to or higher than 1. The critical point is reached for isobutane over HZSM-5(40) and HZSM-5(234), when the isobutane conversion is high (close to 100 and 72%, respectively) and for propane over the most acidic sample, HZSM-5(40), when the propane conversion is 65%.

The initiation of the reaction between NO_2 and hydrocarbons has been proposed to proceed via either a radical type or electrophilic mechanism [64]. The radical type reaction is mostly proposed over transition metal exchanged zeolite systems with either unsaturated or saturated hydrocarbons, and the electrophilic mechanism is demonstrated over acidic zeolite catalysts only for unsaturated hydrocarbons, in particular ethene [30] and propene [29]. The initiation of the SCR reaction with saturated hydrocarbons over acidic zeolite catalysts is not clearly demonstrated in the literature. Burch and Hayes [57] suggested that the activation of the C–H bond over acidic zeolite catalysts proceeds via donation of Brønsted acid protons to the hydrocarbon, forming an adsorbed carbonium ion, which may, in turn, be dehydrogenated to an adsorbed carbenium ion. The subsequent reaction with NO_x can be relatively facile. We have previously suggested formation of the carbenium ions as an important substep in lean NO_x reduction with propane over HZSM-5 [40]. Here this mechanism may also explain the cause of the differences in activity between propane and isobutane. Tertiary carbons (in isobutane) have higher affinity to accept protons leading to more stable tertiary carbenium ions than the secondary carbons in propane.

It is suggested in the literature that when both C, O and N containing adsorbates are formed on the surface, NO_2 can react with these adsorbates and eventually form N_2 [15,16,24]. However, NO_2 will most probably not react directly with adsorbates (following an Eley–Rideal mechanism), instead the adsorbed species containing only N and O (from co-adsorption of $NO_2 + O_2$) likely react with the C, O and N containing adsorbed complexes probably via a Langmuir–Hinshelwood mechanism [15]. Based on in situ spectroscopy we have proposed a reaction path for SCR of NO_2 with propane over the same catalytic system, and we observe the formation of isocyanate and amine species on the catalyst surface [40]. In the present study these species were clearly observed in the in situ DRIFT spectroscopy measurements when isobutane was used as the reducing agent for lean NO_x reduction, over HZSM-5(40) and HZSM-5(234). The growth and decline of these species in the step–response experiments strongly indicate their involvement in the reaction. Furthermore, the corresponding changes in intensity of the Brønsted OH stretching vibrations indicate that these species most likely are formed on the Brønsted acid sites. These observations further support our proposed pathway for the SCR reaction, which most likely starts by the formation of adsorbed carbenium ions and NO^+ species. These species will then further react to form adsorbed isocyanate species, which may hydrolyze with water forming adsorbed amine species. Adsorbed NO^+ species are then likely to react with these amine species to form N_2. In addition, in the present study, species containing –NCO were observed also in the gas phase at 250 °C over the HZSM-5(234) sample, which further support formation of isocyanate or HNCO during the reaction. Acke and Skoglundh [65] reported that HNCO reacted to almost 100% over a Pt/HZSM-5 catalyst above 210 °C for the NO reduction in O_2 excess. Liu et al. [27] observed the emergence of ethyl isocyanate below 330 °C over Cu-MFI under similar conditions when the catalyst became deactivated by surface deposits. This may explain why the –NCO/HNCO species peak at 2280 cm^{-1} was not observed at 350 and 450 °C (in the gas phase) in the present study due to its instability at higher temperature. Furthermore, this peak is not seen in the gas phase over the HZSM-5(40) sample, probably because it is consumed in further reactions as soon as it is formed over this sample.

The obvious difference observed in the DRIFT study between propane and isobutane is the formation of surface adsorbates on the catalysts, which is considerably more pronounced for isobutane than for propane, shown by the formation of broad peaks in the region of 2000–3500 cm^{-1}. This is most likely due to the fact that tertiary carbons in isobutane are considerably easier to activate than secondary carbons in propane, which results in higher coverage of surface adsorbates (saturated and/or unsaturated hydrocarbons) for isobutane.

5. Concluding remarks

The lean reduction of NO_2 by saturated hydrocarbons over acidic HZSM-5 zeolites is strongly dependent on the type of hydrocarbon where isobutane is a more effective reducing agent than propane showing a wider active temperature window, starting at a lower temperature. Key steps in the reaction of NO_2 are likely the formation of NO^+ on the surface and the activation of the hydrocarbon. This is supported by in situ DRIFT studies showing formation of NO^+, isocyanate and amine species on the zeolite surface as well as –CNO/HCNO species in the gas phase during the reaction of NO_2 and isobutane. The differences in reactivity between the two hydrocarbons stem from the fact that the Brønsted acid sites activate isobutane at a lower temperature than propane. This is because the tertiary hydrogen in isobutane is more reactive than the secondary hydrogen in propane. This supports a reaction mechanism for lean NO_2 reduction over acidic zeolites where the hydrocarbon is activated over Brønsted sites forming carbenium ion adsorbates, which may form alkenes that react with NO^+ species forming isocyanate species, amine species and finally nitrogen.

Acknowledgements

The authors would like to thank Dr. Sander van Donk, Albemarle Catalysts BV, for fruitful discussions and for providing the zeolites. This work has been performed within the Department of Chemistry, Göteborg University, and the Competence Centre for Catalysis, which is hosted by Chalmers University of Technology and financially supported by the Swedish Energy Agency and the member companies: AB Volvo, Volvo Car Corporation, Scania AB, GM Powertrain Sweden AB, Haldor Topsøe A/S,

Perstorp AB, Albemarle Catalysts BV and The Swedish Space Corporation.

References

[1] M. Iwamoto, H. Hamada, Catal. Today 10 (1991) 57.
[2] M. Iwamoto, H. Yahiro, S. Shundo, Y. Yu-u, N. Mizuno, Shokubai (Catalyst) 32 (1990) 430.
[3] W. Held, A. Koenig, T. Richter, L. Puppe, SEA Paper 900496 (1990).
[4] H. Hamada, Y. Kintaichi, M. Sasaki, T. Ito, M. Tabata, Appl. Catal. 64 (1990) L1.
[5] H. Hamada, Y. Kintaichi, M. Sasaki, T. Ito, M. Tabata, Appl. Catal. 70 (1991) L15.
[6] Y. Kintaichi, H. Hamada, M. Tabata, M. Sasaki, T. Ito, Catal. Lett. 6 (1990) 239.
[7] I.O.Y. Liu, N.W. Cant, Catal. Surv. Asia 7 (2003) 191.
[8] X. Wang, H.Y. Chen, W.M.H. Sachtler, J. Catal. 197 (2001) 281.
[9] T. Nanba, S. Masukawa, J. Uchisawa, A. Obuchi, Chem. Lett. 33 (2004) 924.
[10] T. Nanba, A. Obuchi, Y. Sugiura, C. Kouno, J. Uchisawa, S. Kushiyama, J. Catal. 211 (2002) 53.
[11] T. Nanba, A. Obuchi, H. Izumi, Y. Sugiura, J.Y. Xu, J. Uchisawa, S. Kushiyama, Chem. Commun. (2001) 173.
[12] N.W. Cant, D.C. Chambers, A.D. Cowan, I.O.Y. Liu, A. Satsuma, Top. Catal. 10 (2000) 13.
[13] H.Y. Chen, X. Wang, W.M.H. Sachtler, Phys. Chem. Chem. Phys. 2 (2000) 3083.
[14] H.Y. Chen, X. Wang, W.M.H. Sachtler, Appl. Catal. A 194 (2000) 159.
[15] H.Y. Chen, T. Voskoboinikov, W.M.H. Sachtler, J. Catal. 186 (1999) 91.
[16] H.Y. Chen, T. Voskoboinikov, W.M.H. Sachtler, Catal. Today 54 (1999) 483.
[17] A.D. Cowan, N.W. Cant, B.S. Haynes, P.F. Nelson, J. Catal. 176 (1998) 329.
[18] T. Beutel, B. Adelman, W.M.H. Sachtler, Catal. Lett. 37 (1996) 125.
[19] B.J. Adelman, T. Beutel, G.D. Lei, W.M.H. Sachtler, Appl. Catal. B 11 (1996) L1.
[20] J.J. Wu, S.C. Larsen, J. Catal. 182 (1999) 244.
[21] E.V. Rebrov, A.V. Simakov, N.N. Sazonova, E.S. Stoyanov, Catal. Lett. 58 (1999) 107.
[22] E.V. Rebrov, A.V. Simakov, N.N. Sazonova, E.S. Stoyanov, Catal. Lett. 64 (2000) 129.
[23] F. Poignant, J.L. Freysz, M. Daturi, J. Saussey, Catal. Today 70 (2001) 197.
[24] H.Y. Chen, T. Voskoboinikov, W.M.H. Sachtler, J. Catal. 180 (1998) 171.
[25] C.A. Jones, S.C. Larsen, Catal. Lett. 78 (2002) 243.
[26] N.W. Cant, A.D. Cowan, A. Doughty, B.S. Haynes, P.F. Nelson, Catal. Lett. 46 (1997) 207.
[27] I.O.Y. Liu, N.W. Cant, B.S. Haynes, P.F. Nelson, J. Catal. 203 (2001) 487.
[28] F. Poignant, J. Saussey, J.C. Lavalley, G. Mabilon, Catal. Today 29 (1996) 93.
[29] T. Gerlach, F.W. Schutze, M. Baerns, J. Catal. 185 (1999) 131.
[30] T. Gerlach, M. Baerns, Chem. Eng. Sci. 54 (1999) 4379.
[31] K. Shimizu, F. Okada, Y. Nakamura, A. Satsuma, T. Hattori, J. Catal. 195 (2000) 151.
[32] F. Radtke, R.A. Koeppel, A. Baiker, Appl. Catal. A 107 (1994) L125.
[33] F. Radtke, R.A. Koeppel, A. Baiker, Environ. Sci. Technol. 29 (1995) 2703.
[34] F. Radtke, R.A. Koeppel, A. Baiker, Chem. Commun. (1995) 427.
[35] F. Radtke, R.A. Koppel, A. Baiker, Catal. Today 26 (1995) 159.
[36] S. Akaratiwa, T. Nanba, A. Obuchi, J. Okayasu, J.O. Uchisawa, S. Kushiyama, Top. Catal. 16 (2001) 209–216.
[37] H. Hamada, Catal. Surv. Jpn. 1 (1997) 53.
[38] T. Holma, A. Palmqvist, M. Skoglundh, E. Jobson, Appl. Catal. B 48 (2004) 95.
[39] J.A. Martens, A. Cauvel, F. Jayat, S. Vergne, E. Jobson, Appl. Catal. B 29 (2001) 299.
[40] H.H. Ingelsten, D. Zhao, A. Palmqvist, M. Skoglundh, J. Catal. 232 (2005) 68.
[41] A. Obuchi, C. Wogerbauer, R. Koppel, A. Baiker, Appl. Catal. B 19 (1998) 9.
[42] A. Hinz, M. Skoglundh, E. Fridell, A. Andersson, J. Catal. 201 (2001) 247.
[43] H.H. Ingelsten, Å. Hildesson, E. Fridell, M. Skoglundh, J. Mol. Catal. A 209 (2004) 199.
[44] K. Hadjiivanov, J. Saussey, J.L. Freysz, J.C. Lavalley, Catal. Lett. 52 (1998) 103.
[45] J. Szanyi, M.T. Paffett, J. Catal. 164 (1996) 232.
[46] M. Trombetta, G. Busca, S. Rossini, V. Piccoli, U. Cornaro, A. Guercio, R. Catani, R.J. Willey, J. Catal. 179 (1998) 581.
[47] G. Boskovic, T. Vulic, E. Kis, P. Putanov, Chem. Eng. Technol. 24 (2001) 269.
[48] B.I. Mosqueda-Jimenez, A. Jentys, K. Seshan, J.A. Lercher, Appl. Catal. B 43 (2003) 105.
[49] M. Wallin, C.-J. Karlsson, A. Palmqvist, M. Skoglundh, Top. Catal. 30/31 (2004) 107.
[50] P.E. Fanning, M.A. Vannice, J. Catal. 207 (2002) 166.
[51] H.H. Ingelsten, M. Skoglundh, E. Fridell, Appl. Catal. B 41 (2003) 287.
[52] NIST Standard Reference Database 69, http://webbook.nist.gov/chemistry, 27 January 2005.
[53] R. Szostak, Molecular Sieves, Van Nostrand Reinhold, New York, 1989.
[54] N.W. Hayes, W. Grunert, G.J. Hutchings, R.W. Joyner, E.S. Shpiro, Chem. Commun. (1994) 531.
[55] S.K. Park, H. Choo, L. Kevan, Phys. Chem. Chem. Phys. 3 (2001) 3247.
[56] F. Solymosi, T. Bansagi, J. Catal. 156 (1995) 75.
[57] R. Burch, M.J. Hayes, J. Mol. Catal. A 100 (1995) 13.
[58] M. Xin, I.C. Hwang, S.I. Woo, J. Phys. Chem. B 101 (1997) 9005.
[59] E. Jobson, A. Baiker, A. Wokaun, J. Chem. Soc. Faraday Trans. 86 (1990) 1131.
[60] N.Y. Topsoe, H. Topsoe, J.A. Dumesic, J. Catal. 151 (1995) 226.
[61] S.K. Park, Y.K. Park, S.E. Park, L. Kevan, Phys. Chem. Chem. Phys. 2 (2000) 5500.
[62] P.B. Weiszs, C.D. Prater, Adv. Catal. 6 (1954) 143.
[63] F. Witzel, G.A. Sill, W.K. Hall, J. Catal. 149 (1994) 229.
[64] R. Brosius, J.A. Martens, Top. Catal. 28 (2004) 119.
[65] F. Acke, M. Skoglundh, Appl. Catal. B 20 (1999) 235.